research articles Journal of proteome research

# Detection of Differential Proteomes Associated with the Development of Type 2 Diabetes in the Zucker Rat Model Using the iTRAQ Technique

**Dohyun Han,[†] Sungyoon Moon,[†] Hyunsoo Kim,[†] Sung-E Choi,[‡] Soo-Jin Lee,[‡] Kyong Soo Park,[§,||] Heesook Jun,[⊥] Yup Kang,*[,‡] and Youngsoo Kim*[,†]**

*Department of Biomedical Sciences, Internal Medicine, and Genome Research Center for Diabetes and Endocrine Disease, Seoul National University College of Medicine, 28 Yongon-Dong, Seoul 110-799 Korea, Institute for Medical Sciences, Ajou University School of Medicine, Wonchon-dong san 5, Suwon, Kyunggi-do, 442-749 Korea, and Lee Gil Ya Cancer and Diabetes Institute, Gachon University of Medicine and Science, Songdo-dong, Incheon 406-840, Korea*

**Received July 23, 2010**

Type 2 diabetes (T2D) is closely associated with obesity, and it arises when pancreatic $\beta$ cells fail to achieve $\beta$ cell compensation. However, the mechanism linking obesity, insulin resistance, and $\beta$ cell failure in T2D is not fully understood. To explore this association, we carried out a differential proteomics study using the disease models of Zucker Fatty (ZF) and Zucker Diabetic Fatty (ZDF) rats as the rat models for obese/prediabetes and obese/diabetes, respectively. Differentially expressed islet proteins were identified among ZDF, ZF, and Zucker Lean (ZL, control rat) rats using three iTRAQ experiments, where three biological replicates and two technical replicates were examined to assess both the technical and biological reproducibilities. A total of 54 and 58 proteins were differentially expressed in ZDF versus ZL rats and in ZF versus ZL rats, respectively. Notably, the novel proteins involved in impaired insulin secretion (Scg2, Anxa2, and Rab10), mitochondrial dysfunction (Atp5b and Atp5l), extracellular matrix proteins (Lgal-1, Vim, and Fbn1), and microvascular ischemia (CPA1, CPA2, CPB, Cela2a, and Cela3b) were observed for the first time. With these novel proteins, our proteomics study could provide valuable clues for better understanding the underlying mechanisms associated with the dynamic transition of obesity to T2D.

**Keywords:** type 2 diabetes • iTRAQ • beta cell • Zucker rat model • obesity

## Introduction

The prevalence of type 2 diabetes (T2D) has risen dramatically; 171 million persons were estimated to have diabetes at the turn of this century.[1] Among several factors associated with the development of T2D, obesity contributes to approximately 55% of T2D.[2] Both obesity and T2D are connected to insulin resistance.[3] Many studies exploring the link between obesity and T2D show that obesity contributes to insulin resistance, resulting in the increase in plasma glucose and fatty acid. In obesity-related insulin resistance, the failure of $\beta$ cell compensation (for example, genetic or acquired factors) results in susceptible pancreatic $\beta$ cells. Subsequently, the increased glucose levels, together with the elevated fatty acid level, synergize to further induce $\beta$ cell dysfunction, $\beta$ cell apoptosis, and impaired glucose tolerance (IGT); the latter is often referred to as "glucolipotoxicity"[4] and precedes the development of hyperglycemia and T2D.

Obesity-related T2D only develops in insulin-resistant subjects with the onset of $\beta$ cell dysfunction after undergoing the processes of $\beta$ cell compensation for insulin resistance in islets.[4−7] Therefore, exploring the mechanisms of islet $\beta$ cell dysfunction is important in obesity-associated T2D.[8] Through extensive experimental evidence obtained *in vitro* and in rodents, the various mechanisms underlying the formation of defective $\beta$ cells remain to be identified.[8−10] For example, impaired glucose-stimulated insulin secretion (GSIS) is induced by a reduction of the glucose-stimulated $Ca^{2+}$ influx and a decrease of ATP generation caused by disorder of glucose metabolism.[11−13] Insulin gene expression is inhibited by a reduction in the binding affinity of $\beta$-cell-specific transcription factors (PDX-1 and MafA).[14,15] The down-regulation of $\beta$-cell-specific transcription factors results in a reduced insulin expression level.[14] A gradual loss of $\beta$ cells due to apoptosis (i.e., programmed cell death) is thought to be induced by

* To whom correspondence should be addressed. Dr. Youngsoo Kim, Department of Biomedical Sciences, Seoul National University College of Medicine, 28 Yongon-Dong, Chongno-Ku, Seoul 110-799 Korea; (Tel) +82-2-3668-7950, (Fax) +82-2-741-0253, biolab@snu.ac.kr. Dr. Yup Kang, Institute for Medical sciences, Ajou University School of Medicine, Wonchon-dong san 5, Youngtong-gu, Suwon, Kyunggi-do, 442-749 Korea; (Tel) +82-31-219-4532, (Fax) +82-31-219-4540, kangy@ajou.ac.kr.

[†] Department of Biomedical Sciences, Seoul National University College of Medicine.

[‡] Ajou University School of Medicine.

[§] Internal Medicine, Seoul National University College of Medicine.

[||] Genome Research Center for Diabetes and Endocrine Disease, Seoul National University College of Medicine.

[⊥] Gachon University of Medicine and Science.


10.1021/pr100759a

Published on Web 12/01/2010

glucolipotoxicity, defined as the combination of excessive levels of fatty acids and glucose. Several studies have proposed that glucolipotoxicity plays a major role in $\beta$ cell death through oxidative stress, ER stress, $Ca^{2+}$-mediated signal transduction, JNK signaling, and lipid-mediated signaling.[4,16,17] However, despite years of investigation and significant progress made in the discovery of the molecular and cellular mechanisms of glucolipotoxicity, its contribution to obesity-related $\beta$ cell dysfunction and death in T2D remains to be discussed.

To further understand the association between insulin resistance, obesity, and $\beta$ cell dysfunction in the development of obesity-associated T2D, we studied the Zucker Diabetic Fatty rat (ZDF) model of T2D. The Zucker Fatty rat (ZF), a model for obese/prediabetes, is characterized by a point mutation in the leptin receptor, and leads to impaired signaling of the leptin receptor, which results in hyperphagia, insulin resistance, hyperinsulinemia, hyperlipoproteinemia, and obesity.[18−20] The ZF rat becomes glucose intolerant but does not develop T2D, whereas the male ZDF rat spontaneously develops T2D.[21] The full syndrome of T2D with hyperglycemia develops in ZDF rats aged 10−12 weeks.[20,22] Several studies comparing ZDF and ZF rats have demonstrated that $\beta$ cell mass dynamics,[23] down-regulation of GLUT2,[24] and mitochondrial dysfunction[25] contribute to $\beta$ cell failure and the development of T2D in ZDF rats.[8]

Because the morphology, metabolism, and function of any cell are primarily determined by the entire population of cellular proteins, the identification of underlying mechanisms linking obesity to insulin resistance and T2D should be focused on the protein composition and changes of expression level. Differential proteomics has been developed to investigate molecular changes and has been applied to studies of T2D on various cell lines and tissue, such as adipose tissue,[26] skeletal muscle,[27] liver,[28] and even semen.[29] However, extensive and/or comparative proteomic studies of islets to explore the mechanisms underlying insulin resistance, the key features of obesity, and T2D have not yet been undertaken. Only limited information is available concerning the differential proteomic changes in pancreatic islets to link insulin resistance, obesity, and $\beta$ cell dysfunction in the development of T2D.[30]

Therefore, we investigated the molecular mechanisms linking obesity to insulin resistance, $\beta$ cell dysfunction and failure, and T2D. We applied iTRAQ labeling coupled with offline 2D LC−MS/MS proteomics technology to quantitatively analyze the protein expression profile of the Zucker rat models (Zucker lean, Zucker Fatty, and Zucker Diabetic Fatty rats).[31,32] Analysis of differential proteome was performed using islets isolated from 14-week-old ZL, ZF, and ZDF rats. A total of 54 proteins were differentially expressed in the comparison of ZDF versus ZL rats. A total of 58 proteins provided quantitative information in the comparison of ZF versus ZL rats. Clustering analysis of the differentially expressed proteins was performed to explore the relationships between obesity, insulin resistance, and $\beta$ cell failure.

Interestingly, our iTRAQ study suggested that novel proteins involved in impaired insulin secretion, mitochondria dysfunction, dysregulation of triglyceride/free fatty acid cycling and lipotoxicity, extracellular matrix proteins, and microvascular ischemia, which were identified for the first time, may be related to $\beta$ cell failure and the development of obesity-related T2D. Besides, functional clustering analysis demonstrated the up-regulation of protein metabolism and modification, and the down-regulation of mitochondrial energy metabolism, as previously proposed in T2D. Consequently, this differential proteomic study for ZDF and ZF rats provided functional implications of the molecular changes associated with the dynamic transition of obesity to T2D.

## Materials and Methods

**Zucker Rat Models.** The 7-week-old male Zucker Diabetic Fatty (ZDF), male Zucker Fatty (ZF), and male Zucker Lean (ZL) rats were purchased from Charles River Laboratories (Wilmington, MA). The rats were housed singly in isolation cages and kept at a constant temperature of 22−23 °C in humidity-controlled rooms on a standard 12/12-h light−dark cycle. The rats were fed water and Purina 5001 chow ad libitum throughout the experiment. The experiments were carried out in accordance with the guidelines of the Animal Care Committee of the Ajou University School of Medicine.

The oral glucose tolerance test (OGTT) and insulin quantitation assay of each Zucker rat were performed using the method described in the Supplementary Methods.

**Immunohistochemistry.** For the detection of insulin, deparaffinized pancreatic sections were blocked with 10% rabbit serum in phosphate saline for 10 min and subsequently overlaid with a guinea pig anti-insulin antibody (DAKO, Carpinteria, CA) diluted 1:500 in blocking buffer for 3 h. After the biotinylated rabbit anti-guinea pig IgG antibody was applied, the sections were treated with streptavidin-conjugated horseradish peroxidase (DAKO, Carpinteria, CA). Immunoreactions were visualized by the addition of peroxidase substrate solution containing 3,3′-diaminobenzidine tetrahydrochloride (DAB).

**Isolation of Islets.** Islets were isolated from male ZL, ZF, and ZDF rats aged 12−14 weeks using the collagenase digestion method. Briefly, after injecting 10 mL of collagenase P (0.75 mg/mL) into the bile ducts, the swollen pancreases were excised and then incubated in a water bath at 37 °C for 7 min. After the enzymatic digestion was stopped with cold Hanks' balanced salt solution (HBSS), the tissues were disrupted by repetitive pipetting and then were passed through a 400 Φ mesh. The islets were separated by centrifugation on 25%, 23%, 21.5%, and 11.5% Ficoll gradients. Islets at the interface between the 21.5% and 11.5% fractions were collected and washed with HBSS. Healthy islets were hand-picked under a stereomicroscope.

**iTRAQ Sample Preparation.** For three iTRAQ experiments, islets isolated from 2−3 Zucker rats were pooled. The islets were lysed several times by freeze−thawing, followed by sonication. The extracted proteins were reduced, alkylated, digested, and labeled with iTRAQ-reagents as described in the iTRAQ protocol (Applied Biosystems, Foster City, CA). Additional details of iTRAQ sample preparation are provided in Supplementary Methods.

**Peptide Fractionation, LC−MS/MS Acquisition, And Data Processing.** Labeled peptides were subjected to offline strong cation exchange (SCX) fractionation and then to C18 chromatography coupled directly to a hybrid Quadrupole-TOF LC−MS/MS spectrometer (QStar Elite; Applied Biosystems). Detailed procedures of the peptide fractionation, data acquisition, and processing are described in the Supplementary Methods.

**Data Analysis.** Database searches to identify the peptides were performed with ProteinPilot 2.0.1 software (Applied Biosystems) using the Paragon and ProGroup algorithms against the IPI rat database (IPI.rat.v3.69, 39 578 entries). Additional details of the quantitative data analysis are described

**Table 1.** Weight, Blood Glucose, And Insulin in Zucker Rats

| animals (number) | weight (g) | fasting glucose (mg/dL) | glucose after 2 h glucose challenge (mg/dL) | fasting insulin (ng/mL) | insulin after 2 h glucose challenge (ng/dL) |
|---|---|---|---|---|---|
| 9-week-old ZDF (10) | 324.2 + 4.4 | 118.2 + 4.8 | 168.0 + 7.7 | 2.7 + 0.6 | 3.9 + 0.6 |
| 14-week-old ZDF (12) | 446.5 + 3.9 | 159.6 + 15.2 | 281.4 + 26 | 4.6 + 0.7 | 7.1 + 1.0 |
| 14-week-old ZF (6) | 523.7 + 10.1 | 157.3 + 8.6 | 193.5 + 13.5 | 8.7 + 2.1 | 30.1 + 2.2 |
| 14-week-old ZL (8) | 332.8 + 4.4 | 90.6 + 2.5 | 117.6 + 5.2 | 0.8 + 0.2 | 0.6 + 0.1 |

in Supplementary Methods. Briefly, for quantitative, differentially expressed proteins, we selected proteins using the following criteria: (1) the proteins must contain at least two unique high-scoring peptides (peptide confidence >90%); (2) the EF must be below 2, and the relative quantification *p*-values must be below 0.05, in each biological replicate; (3) proteins with high CV values are removed; (4) quantitative proteins must be observed across two of the three biological replicates.

**Western Blotting.** The changes in the expression of insulin (INS), carboxylpeptidase E (CPE), carboxylpeptidase A1 (CPA1), galectin-1 (LGAL1), and vimentin (VIM) were validated by Western blotting to verify the results obtained by iTRAQ analysis. Protein extraction and Western blotting were carried out using the procedure described in the Supplementary Methods.

## Results

**Characteristics of Zucker Rat Models.** To obtain insights into the molecular differences during the changes occurring either from normal to obesity or from obesity to diabetic islets, we investigated differential proteomes between normal, obese/prediabetic, and obese/diabetic rat islets; the rats were 14-week-old Zucker Lean (ZL), 14-week-old Zucker Fatty (ZF), and 14-week-old Zucker Diabetic Fatty (ZDF), respectively. The average weight of ZDF rats at 14 weeks of age was 446.5 g; rats at 9 weeks of age weighed an average of 324.2 g. The average weights of ZF and ZL rats at 14 weeks were 523.7 and 332.8 g, respectively. Since both ZDF and ZF at 14 weeks were much heavier than the control ZL rat, the ZDF and ZF rats were used as obese subjects; ZL was normal (Table 1). The glucose levels at 120 min after a glucose challenge (2 g/kg) were 168.0, 281.4, 193.5, and 117.6 g/dL in the 9-week-old ZDF, 14-week-old ZDF, 14-week-old ZF, and 14-week-old ZL rats, respectively. Because 2 h plasma glucose ≥200 mg/dL (11.1 mmol/L) during an OGTT meets the threshold for the diagnosis of diabetes,[33] our OGTT results demonstrate that the 14-week-old ZDF rat was obviously diabetic and that the 14-week-old ZF rat was prediabetic, while the 9-week-old ZDF and 14-week-old ZL rats were nondiabetic (Table 1). The levels of fasting insulin were 2.7, 4.6, 8.7, and 0.8 ng/mL in the 9-week-old ZDF, 14-week-old ZDF, 14-week-old ZF, and 14-week-old ZL rats, respectively. However, the insulin levels after the 2 h glucose challenge were 3.9, 7.1, 30.1, and 0.6 ng/mL in the 9-week-old ZDF, 14-week-old ZDF, 14-week-old ZF, and 14-week-old ZL rats, respectively. These data demonstrated that the insulin levels were higher in obese subjects, possibly for compensating insulin resistance (Table 1). The insulin level after the glucose challenge was dramatically increased only in the 14-week-old ZF rat. Insulin immunohistochemistry showed that the islets were heavily expanded in both the ZDF and ZF rats, compared to the ZL rat, suggesting that islet hyperplasia existed in obese ZDF and ZF (Figure 1). The islet of the 14-week-old ZDF rat was disorganized, with expansion into adjacent tissues, while the islet of 14-week-old ZF rat was elongated. However, the islet of 9-week-old ZDF rat was well organized and round in shape. Insulin-positive cells were irregularly scattered in the 14-week-old ZDF rat. The staining intensity of insulin was weaker in ZDF and ZF islets than in ZF islets. The $\beta$ cell integrity was lost in the obese/diabetic ZDF rat, whereas that of obese/prediabetic ZF rats was relatively intact, although both rat islets had common hyperplasia patterns.

**iTRAQ Analysis of Islets from Zucker Rat Models.** To gain insights into the underlying relationship between obesity and T2D, we applied the iTRAQ technique coupled with 2D-nano LC/MS/MS to quantitatively identify the global differential proteomes of Zucker rat islets. To identify the differential proteomes whose expression levels were either up- or down-regulated during the development of T2D in obese Zucker rat models, islets of ZF, ZDF, and ZL rats were subjected to iTRAQ experiments; thereafter, 2D LC/MS/MS were carried out as described in the Materials and Methods and the Supplementary Methods (Figure 2A).

The iTRAQ experiments were performed as three independent biological replicates to gather reliable quantitative information (Figure 2B). In addition, the same 114 tag-labeled sample using 9-week-old ZDF was analyzed repeatedly in the biological replicates #1 and #2 and used as two technical replications. Comparison set #1 was utilized to assess technical replications. These two technical replications were included in the total profiling of the proteome to enhance protein coverage, but they were not used for the quantitative analysis of the differentially expressed proteome. In contrast, quantitative

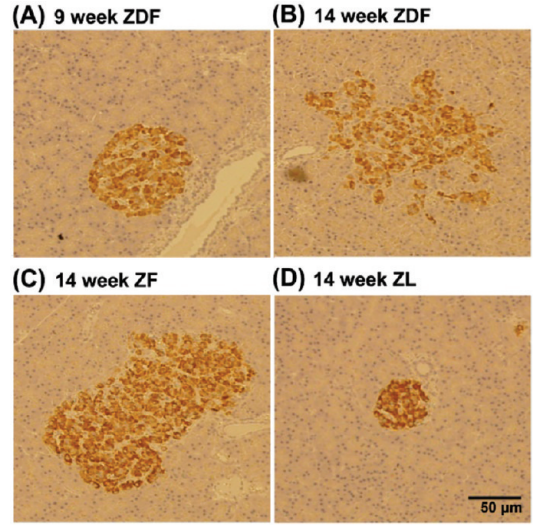


**Figure 1.** Immunohistochemistry of insulin-positive islets Pancreatic sections were incubated with anti-rat insulin antibody, stained with the peroxidase/DAB system, and observed under a microscope (original magnification ×200). Bar = 50 $\mu$m. Panels show representative images obtained from (A) 9-week-old ZDF, (B) 14-week-old ZDF, (C) 14-week-old ZF, and (D) 14-week-old ZL rats.

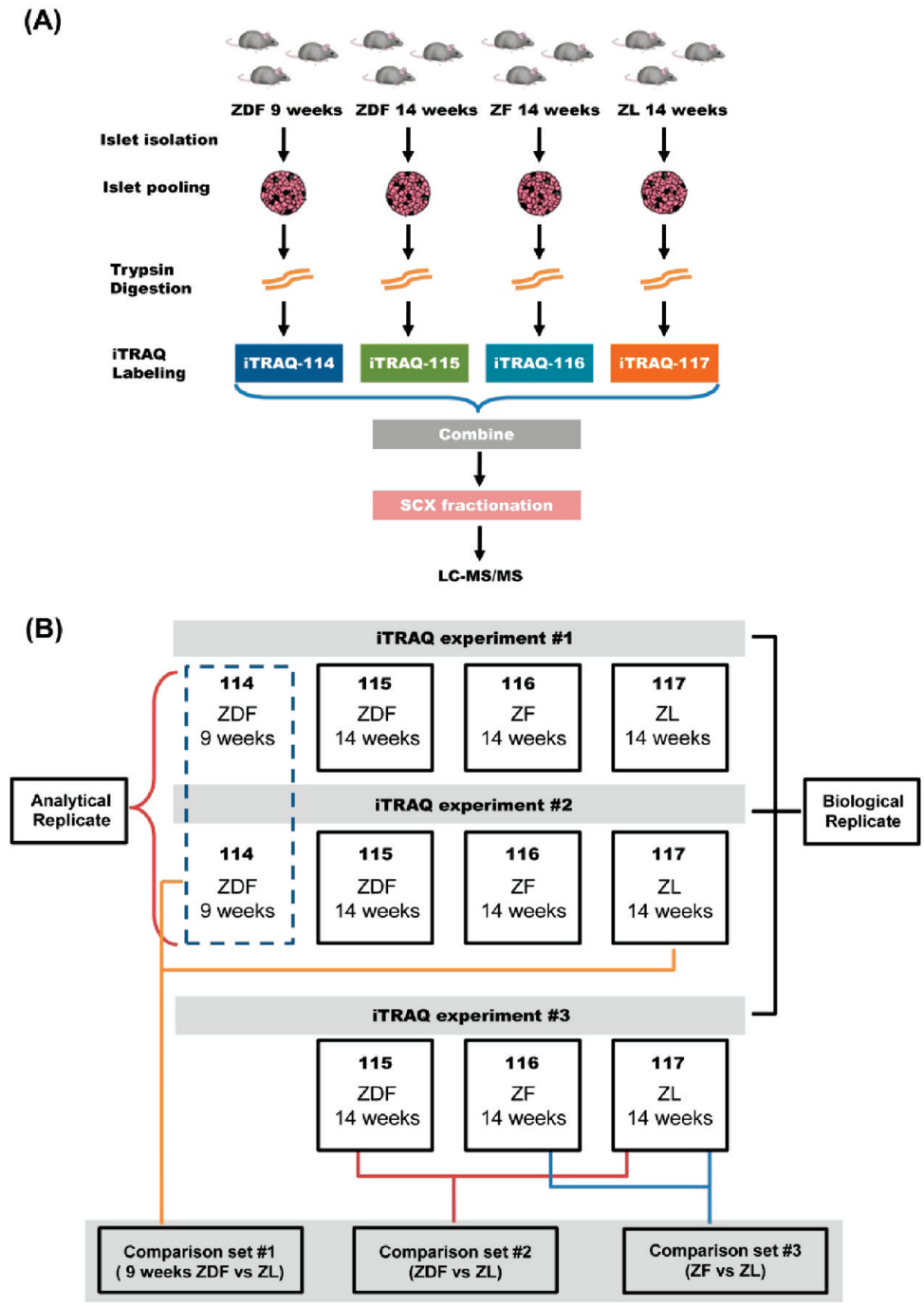


**Figure 2.** Quantitative iTRAQ proteomics approach. (A) Sample preparation of the Zucker rat models for iTRAQ experiments. (B) Strategy for performing iTRAQ analysis using the Zucker rat models. Pooled islets from 14-week-old ZL, 14-week-old ZDF, and 14-week-old ZF rats were measured as three biological replicates in three iTRAQ experiments, while 9-week-old ZDF rats were measured as two technical replicates in two iTRAQ experiments.

analysis used comparison sets #2 and #3 obtained using the three biological replications.

**Protein Identification of Zucker Rat Islets.** The information from the three iTRAQ experiments was analyzed using the ProteinPilot search algorithm[34] against the IPI rat database (IPI.rat.v3.69, with 39 578 entries). From the three iTRAQ experiments, 22 643, 14 267, and 10 366 MS/MS spectra were identified, leading to identification of 13 495, 8574, and 6052 distinct peptides with 95% confidence, respectively. After the redundancies were removed using the criteria for protein identification mentioned in the Materials and Methods, a total of 1084 unique proteins were identified in all three individual iTRAQ experiments (Supplementary Table S1). In fact, 234 (21.5%) of these 1084 proteins were shared by all three iTRAQ experiments, and 241 (22%) were shared by two experiments; thus, about half (475 of 1084 proteins) of the identified proteins were detected in at least two of the three iTRAQ experiments (Supplementary Figure S1A). Of all proteins that were identified by the three iTRAQ experiments, about 40% of the total identified proteins were obtained by single peptide. This is

likely due to the complexity and existence of abundant proteins in the islets. Approximately 25% of the total identified proteins were obtained by more than five peptides, which indicated that these portions of proteins are mainly abundant proteins (Supplementary Figure S1B).

A total of 1084 proteins from the three iTRAQ experiments were categorized according to their molecular functions using the DAVID server[35] (Supplementary Figure S1C). Of the total, the proteins involved in binding and catalytic activity were 75.7% and 35.2%, respectively. The remaining proteins were categorized into structural molecule activity, transporter activity, enzyme regulator activity, molecular transducer activity, electron carrier activity, antioxidant activity, proteasome regulator activity, and translation regulator activity, respectively.

**Examining the Technical and Biological Reproducibilities of Three iTRAQ Experiments.** Three biological replicates in the three iTRAQ experiments were evaluated to minimize the influence of less reliable quantitative information and also to improve the coverage of differentially expressed proteins. Briefly, 100 $\mu$g of islet proteins from 14-week-old ZDF, 14-week-old ZF, and 14-week-old ZL rats was labeled with iTRAQ reagents 115, 116, and 117, respectively; then, the three iTRAQ experiments (#1, #2, and #3) were carried out.

In addition, two technical replicates of the iTRAQ experiment, #1 and #2, were performed to examine the random errors of the iTRAQ experiments. For the two technical replicates, 200 $\mu$g of the same islet proteins from the 9-week-old ZDF rats was labeled with iTRAQ reagent 114 and divided into 2 samples of 100 $\mu$g each so that the two technical replicate iTRAQ experiments #1 and #2 could be carried out (Figure 2B).

To determine the cutoff value of the significant differential fold change, the iTRAQ ratios for 9-week-old ZDF versus 14-week-old ZL rats (comparison set #1; 114/117), 14 week-old ZDF versus 14-week-old ZL rats (comparison set #2; 115/117), and 14-week-old ZF versus 14-week-old ZL rats (comparison set #3; 116/117) were compared in each respective comparison set (Figure 2B). The significantly quantifiable proteins that satisfied the confidence interval (CI) >95%, EF value <2, and at least two peptide requirements were used to calculate the coefficients of variation (CV) in each comparison set. The CV distributions of the three comparison sets (#1, #2, and #3) were used to estimate and therefore determine the cutoff values for meaningful fold changes in each comparison set.

For example, in comparison set #1 of the two technical replicates, a total of 123 proteins were commonly identified as the proteins between the two iTRAQ experiments #1 and #2 that satisfied the criteria of significantly quantifiable proteins (Figure 2B). Ninety percent of the 123 identified proteins in comparison set #1 fell within 25% of the CV (Supplementary Figure S2A). Therefore, we decided that a fold change of $\geq 1.25$ or $\leq 0.8$ would be the meaningful cutoff representing significant differences in the differential proteome in the iTRAQ experiments #1 and #2.

The distribution of the CV values for three biological replicates was also examined by analyzing comparison sets #2 and #3. In comparison set #2, a total of 520 proteins were identified as the proteins from the three iTRAQ experiments (#1, #2, #3) using the quantifiable criteria mentioned above. Among the 520 candidate proteins, 91 proteins were commonly identified in all three iTRAQ experiments. In comparison set #3, a total of 535 proteins were identified as quantifiable proteins from the three iTRAQ experiments (#1, #2, #3), where 99 proteins were common to all three iTRAQ experiments. Those commonly identified 91 and 99 proteins in comparison sets #2 and #3 were used in calculating the CV distribution (Supplementary Figure S2B). The results showed that about 90% of proteins of comparison sets #2 and #3 had a CV value of less than 25%, which suggested that those three iTRAQ experiments showed good experimental reproducibility in both the two technical replicates and three biological replicates. Since 90% of the commonly quantifiable proteins in comparison sets #2 and #3 fell within 25% and 20% of the CV values, we determined that the values of significant differential fold change of $\geq 1.25$ or $\leq 0.8$ (comparison set #2) and $\geq 1.2$ or $\leq 0.83$ (comparison set #3) were meaningful cutoffs representing differential proteomes in the three iTRAQ experiments.

We applied the following stringent criteria to obtain a list of quantified proteins from the three iTRAQ experiments with three biological replicates: (1) the proteins are identified by at least two biological replicates; (2) for comparison set #2, the iTRAQ ratios must be higher than 1.25 or lower than 0.8, but for comparison set #3, the iTRAQ ratios must be higher than 1.2 or lower than 0.83; (3) the *P*-values of the iTRAQ ratios must be less than 0.05 in three biological replicates; and (4) proteins with a high CV value (more than 60%) are not included.

Furthermore, the consistency of the three iTRAQ experiments was cross-checked using the full list of the quantified proteins selected from comparison sets #2 and #3 with the above stringent selection criteria. Linear regression analyses were performed on ln-transformed iTRAQ ratios between all three iTRAQ experiments (Supplementary Figure S3). Pearson correlation coefficients (*R*-value) for comparison set #2 were 0.929 between iTRAQ experiments #1 and #2, 0.893 between iTRAQ experiments #1 and #3, and 0.927 between iTRAQ experiments #2 and #3, respectively ($p \leq 0.0001$). The corresponding *R*-values in comparison set #3 were 0.907, 0.834, and 0.908, respectively ($p \leq 0.0001$). Therefore, our three iTRAQ experiments demonstrated reliable reproducibility in both the technical and biological replicate sets.

**Differentially Expressed Proteins between ZDF and ZL Islets.** A total of 162 proteins were quantified in ZDF versus ZL rats with a $\leq 0.8$ or $\geq 1.25$ fold change. In total, 54 proteins were identified in at least two of the three biological replicates (Supplementary Table S2), whereas 14 proteins appeared in all three biological replicates. Thirty proteins among the 54 proteins were found to be significantly up-regulated, and the other 24 proteins were down-regulated (Supplementary Table S2).

To gain insights into the biological changes of the differential proteome in the ZDF versus ZL rat model during the progress of obese/prediabetic to obese/diabetic state, the differentially expressed proteins were categorized according to the Gene Ontology (GO) classes "cellular component", "molecular functions", and "biological process". To obtain a general GO classification, the DAVID server[35] and the AmiGo server[36] were utilized to search the GO database. In addition, the remaining proteins that are not yet annotated in the GO database were categorized according to the main functions collected from the UniProt protein knowledge database (http://www.uniprot.org) and from PubMed (http://pubmed.gov).

In the cellular component of GO analysis, the highest proportion of differentially expressed proteins was located in the extracellular region (30%). Proteins located in the mitochondria (22%) and the cytoskeleton (13%) were the next two largest groups in the ZDF islet (Figure 3A). Classification analysis based on the molecular functions of GO analysis

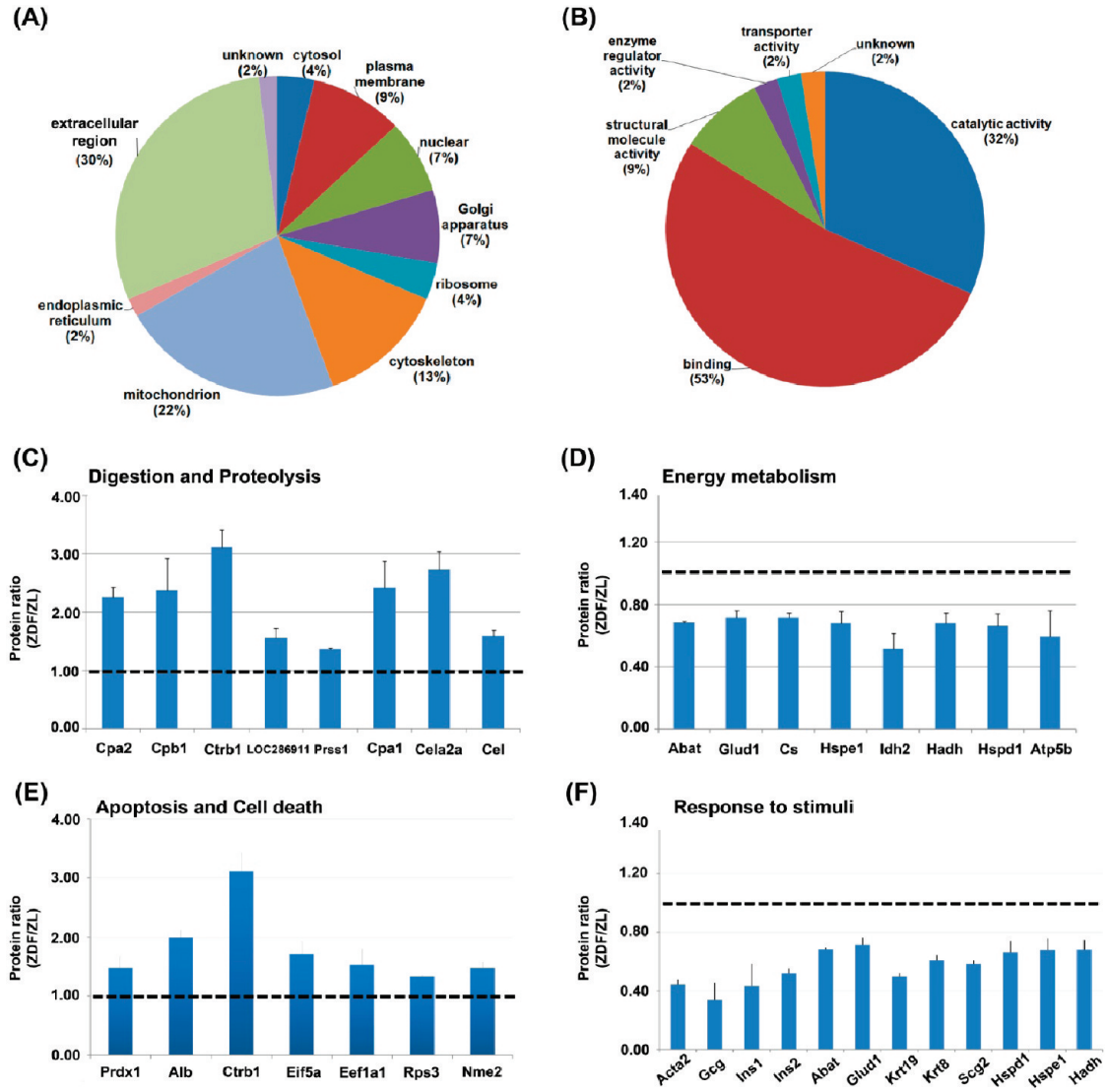


**Figure 3.** Functional categorization and relative ratios of differentially expressed proteins in ZDF versus ZL islets. GO classification of proteins quantified in comparison set #2 based on (A) cellular component and (B) molecular functions. Relative changes in the proteins differentially expressed in ZDF versus ZF islets are associated with (C) digestion and proteolysis, (D) energy metabolism, (E) apoptosis and cell death, and (F) response to stimuli. The dashed lines represent an iTRAQ ratio of 1.0.

revealed that the majority of changed proteins in ZDF versus ZL islets were associated with two major functions, namely, binding (53%) and catalyst activity (32%) (Figure 3B). In addition, the GO analysis of biological process revealed that the up-regulated proteins comprised subcategories of protein metabolism and modification, lipid metabolism, cell development, nucleoside, nucleotide and nucleic acid metabolism, transport, and carbohydrate metabolism (Supplementary Table S2). Moreover, the down-regulated proteins fell into the six following biological process subcategories: energy metabolism, cytoskeleton, transport, cell development, protein metabolism, and nucleosome assembly (Supplementary Table S2).

Among the up-regulated proteins, the most overrepresented processes in the biological process subcategory of the GO analysis were involved in proteolysis and digestion, apoptosis and cell death, and protein biosynthesis. In contrast, the down-regulated proteins comprised the hallmark mitochondrial defect and a group of proteins that respond to stimuli. Figure 3C−F lists the representative differentially expressed proteins in ZDF versus ZL rats, related to digestion and proteolysis (Cpa1, Cpa2, Cpb1, Ctrb1, LOC286911, Prss1, Cela2a, and Cel), apoptosis and cell death (Prdx1, Alb, Ctrb1, Eif5a, Eef1a1, Rps3, and Nme2), energy metabolism (Abat, Glud1, Cs, Hspe1, Idh2, Hadh, Hspd1, and Atp5b), and response to stimulus (Acta2, Gcg, Ins1, Ins2, Abat, Glud1, Krt19, Krt18, Scg2, Hspd1, Hspe1, and Hadh), respectively.

**Differentially Expressed Proteins in ZF versus ZL Rats.** A total of 175 proteins were quantified using the previously mentioned stringent criteria in ZF versus ZL rats; 58 proteins were identified in at least two of the three biological experiments (Supplementary Table S3), while 15 proteins appeared in all three biological replicates. Only in comparison set #3 (ZF versus ZL rats), the cutoff values for down- and up-regulated proteins were ≤0.83 or ≥1.2 (Supplementary Figure S2B). Among the 58 proteins quantified in two of the three biological experiments, 31 proteins were significantly up-regulated and the other 27 proteins were down-regulated (Supplementary Table S3).

To investigate the molecular consequences of the progress of obesity in ZF compared to the ZL rat model, differentially

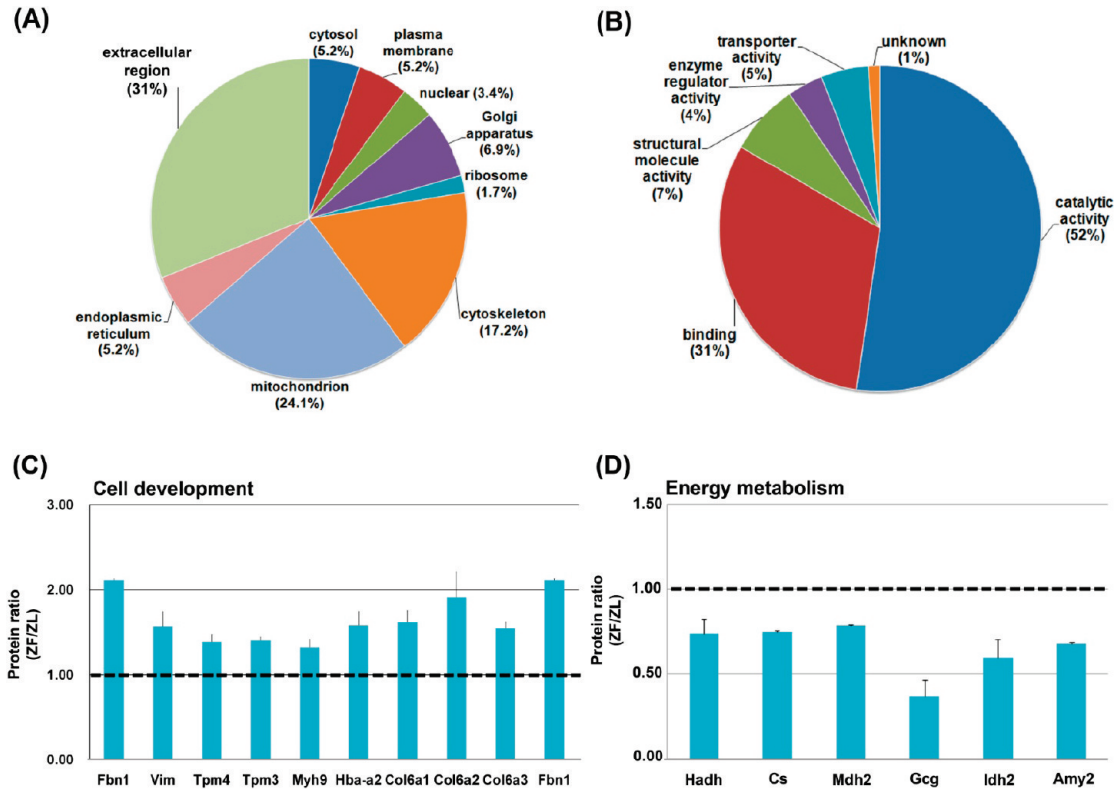


**Figure 4.** Functional categorization and relative ratios of differentially expressed proteins in ZF versus ZL islets. GO classification of proteins quantified in comparison set #3 based on (A) cellular component and (B) molecular functions. Relative changes in the proteins differentially expressed in ZF versus ZL islets are associated with (C) cell development and (D) energy metabolism. The dashed lines represent an iTRAQ ratio of 1.0.

expressed proteins were categorized into cellular component, molecular functions, and the biological process of GO analysis as described above for the ZDF versus ZL rats. As for ZDF versus ZL rats, GO analysis of cellular component shows that the highest proportion of differentially expressed proteins was located in the extracellular region (31%). This observation was similar to that in ZDF versus ZF rats (Figure 4A). Moreover, the GO analysis of molecular functions revealed that the majority of differentially expressed proteins in ZF versus ZL rats were also associated with binding (31%) and catalyst activity (52%); the latter pattern was similar to that of ZDF versus ZF rats (Figure 4B).

The GO analysis of biological process revealed that the up-regulated proteins comprised subcategories of protein metabolism and modification; cell development; nucleoside, nucleotide, and nucleic acid metabolism and transport; and carbohydrate metabolism (Supplementary Table S3). In addition, the down-regulated proteins were sorted into the following seven subcategories: energy metabolism, cytoskeleton, transport, cell development, protein metabolism, signal transduction, and nucleosome assembly (Supplementary Table S3).

Interestingly, the GO analysis of biological process showed that a particular difference exists between ZDF versus ZL rats (115/117) and ZF versus ZL rats (116/117). In ZF versus ZL rats, the largest fraction of up-regulated proteins was associated with cell development and with protein metabolism and modification. In fact, many extracellular matrix (ECM) proteins included in the cell development process are identified. However, the down-regulated proteins were almost confined to energy metabolism, as for the ZDF versus ZL rats. Figure 4C,D shows the representative differentially expressed proteins related to cell development (Fbn1, Vim, Tpm4, Tpm3, Myh9, and Hba-a2) and energy metabolism (Hadh, Cs, Mdh2, Gcg, Idh2, and Amy2) in ZF versus ZL rats.

**Clustering Analysis for Differentially Expressed Proteins in ZDF versus ZF Rats.** To investigate the molecular changes from obese prediabetes to obese diabetes, we applied the methods of hierarchical clustering and manual grouping to the differential proteome, which consisted of the 65 proteins commonly identified in both ZDF versus ZL (115/117 tag) and ZF versus ZL (116/117 tag). The averaged ratios indicated the reporter ion intensity derived from the ZDF (iTRAQ-115) and ZF (iTRAQ-116) versus ZL (iTRAQ-114) proteins. The mean iTRAQ ratio of each protein was used to perform the cluster analysis based on Pearson correlations using the Cluster 3.0 program[37] and were visualized using the Java TreeView program[38] (Figure 5A). The hierarchical clustering analysis revealed that the 65 proteins were clustered together into six major patterns of expression, based on the differentially expressed patterns over the progress of diabetes from normal (ZL) to prediabetic (ZF) and finally to diabetic (ZDF) islets (Supplementary Table S4). The expression pattern of each differentially expressed protein over the development of diabetes could be easily recognized in Figure 5B.

Interestingly, the six patterns of differential expressions revealed divergent protein expression during the progress of diabetes. For example, Cluster 1, which contained elongation factor 1-alpha1 (Eef1a1), elongation factor 2 (Eef2), nucleoside diphosphate kinase B (Nme2), and coatomer subunit beta (Copb1), showed a slight increase in ZDF rats compared to ZF and ZL rats. In Cluster 2, a total of 13 proteins were significantly up-regulated in the ZDF rat compared to the ZF rat; most of

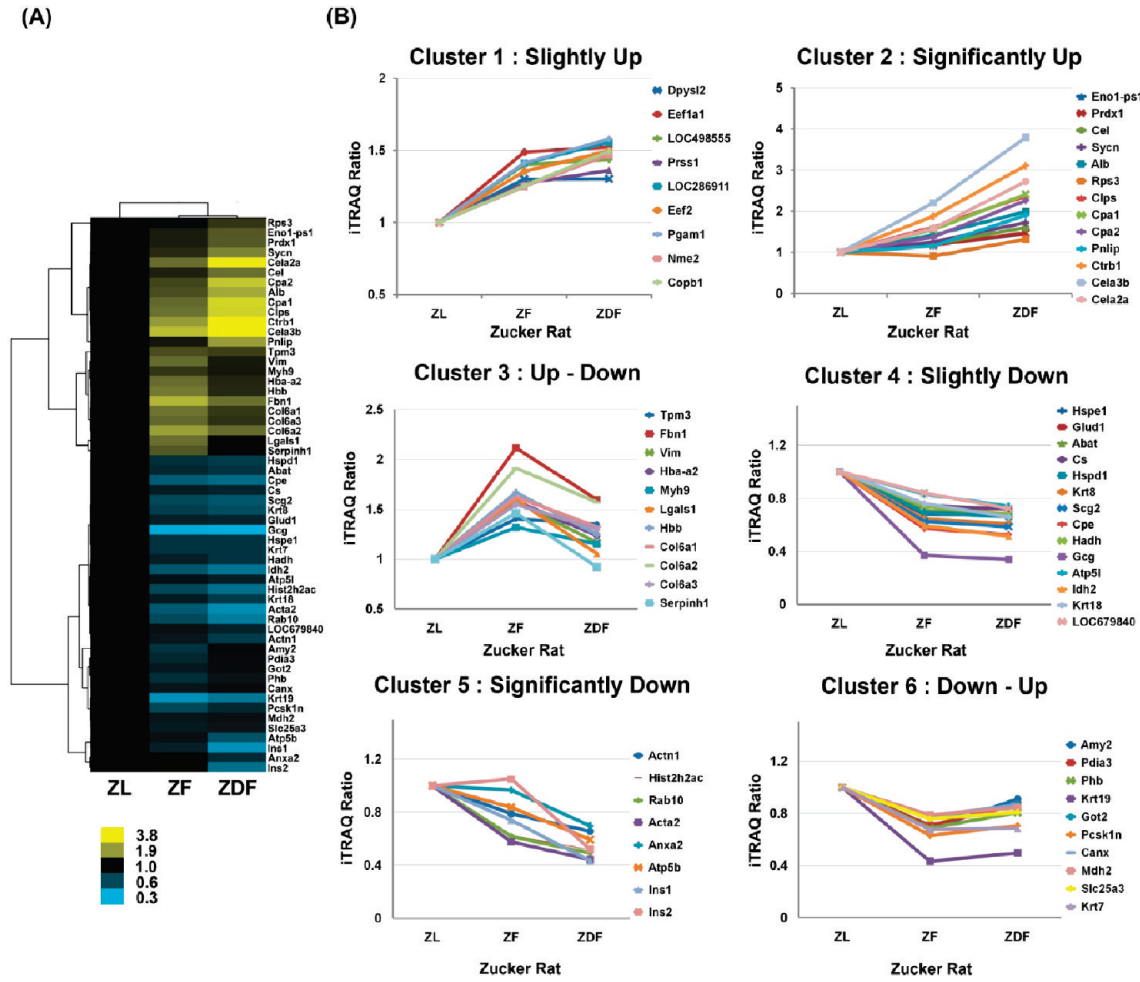


**Figure 5.** Hierarchical clustering for differentially expressed proteins in Zucker rat models. Hierarchical clustering was performed with Pearson correlations on the proteins used to generate the heat map using the Cluster 3.0 program.[37] (A) An overview of clustering; the color gradient bar represents a scale of 3.8 to 0.3 from yellow to blue for the iTRAQ ratios. The proteins in clusters exhibit progressive up- or down-regulated patterns during the progress of diabetes and were grouped into six representative clusters, Clusters 1−6. (B) Hierarchical clustering resulted in six clusters as detailed in Supplementary Table S4.

these proteins belonged to digestion and proteolysis. In Cluster 4, 14 proteins were slightly down-regulated in both ZF and ZDF rats; here, the proteins were mainly related to energy metabolism, especially mitochondrial metabolism. In Cluster 5, proteins containing insulin (Ins1 and Ins2), glucagon (Gcg), ATP synthase subunit beta (Atp5b), and Rab10, a member of the RAS oncogene family (Rab10), showed a dramatic decrease in ZDF rats versus ZF and ZL rats.

However, the proteins found in Cluster 3 (Tpm3, Fbn1, Vim, Hba-a2, Myh9, Lgals1, Hbb, Col6a1, Col6a2, Col6a3, and Serpinh1) showed a significant increase in the ZF rat and then returned to the control ZL level in the ZDF rat. Interestingly, Cluster 3 represents ZF-specific elevated proteins, which mostly belong to ECM proteins. In contrast, Cluster 6, which included pancreatic alpha-amylase (Amy2), protein disulfide-isomerase A3 (Pdia3), and prohibitin (Phb), showed a dramatic decrease in the ZF rat and then stayed at the same level as that of the ZDF rat.

**Validation of Differentially Expressed Proteins by Western Blotting.** To validate the differentially expressed proteins obtained from the iTRAQ-based quantitative proteomics study, Western blotting was performed on pooled islets of ZL, ZF, and ZDF rats. According to the clustering analysis for expression patterns, the significantly down-regulated protein (insulin [INS]), slightly down-regulated protein (carboxylpeptidase E [CPE]), up−down proteins (vimentin [VIM] and galectin-1 [LGAL1]), and significantly up-regulated proteins (carboxylpeptidase A [CPA]) were validated by Western blotting; representative Western blots are shown with quantification data (Supplementary Figure S4). To investigate the relationship between the expression ratios detected by Western blotting and the iTRAQ experiments, the band intensities of the Western blotting results were quantified using the densitometric software Multi Gauge (Fuji, Tokyo, Japan).

Compared to the ZL rat, insulin expression decreased dramatically in the ZDF rat (Supplementary Figure S4). Although the respective iTRAQ ratios of CPA are 1.00/1.55/2.41 in the ZL, ZF, and ZDF rats, the densitometric analysis exhibited the ratios of 1.00/1.071/1.43, where only the ZDF rat showed the increment. In addition, LGAL1 and VIM were up-regulated compared to ZL and ZDF rats. The densitometry ratios of LGAL1 (1.00/1.304/1.127 in the ZL, ZF, and ZDF rats, respectively) and VIM (1.00/1.442/1.274 in the ZL, ZF, and ZDF rats) were consistent with the iTRAQ ratios of LGAL1 (1.00/1.60/1.05 in the ZL, ZF, and ZDF rats) and VIM (1.00/1.57/1.16 in the ZL, ZF, and ZDF rats).

However, the densitometry ratios (1.00/1.51/0.90 in the ZL, ZF, and ZDF rats) of CPE showed an increase in the ZF rat and returned to a level below that of the ZL rat, whereas the iTRAQ ratios were 1.00/0.57/0.53 in the ZL, ZF, and ZDF rats. Although the exact changes were slightly different, a large portion of the expression patterns was consistent among two distinct methods overall.

## Discussion

**Differential Proteome Study in ZDF versus ZF Rats.** Obesity has led to a dramatic increase in the incidence of T2D among children and adolescents over the past two decades.[39] Although the mechanism underlying $\beta$ cell failure in most forms of T2D has been elucidated,[8] the mechanisms linking obesity, insulin resistance, and type 2 diabetes are still unclear.

The obese Zucker Fatty (ZF) and obese Zucker Diabetic Fatty (ZDF) rats are characterized by a single point mutation of the leptin receptor.[20] Although the ZDF rat has the same leptin receptor mutation and similar levels of hyperphagia, obesity, and hyperlipidemia as the ZF rat, males spontaneously develop diabetes.[20,22] Therefore, the ZDF rat provides a precise model for T2D based on impaired glucose tolerance (IGT) caused by the inherited obesity gene mutation that leads to insulin resistance and $\beta$ cell dysfunction.[8,20] The fact that the ZF rat is capable of long-term $\beta$ cell compensation with the maintenance of normoglycemia suggests that additional factors are involved in $\beta$ cell failure in ZF versus ZDF rats.[8] To unravel the mechanism linking obesity to the development of T2D, proteomic profiling should be the preferred choice; previous large-scale studies on the association with obesity and T2D were mainly restricted to the transcriptome level.[40] Although a few large-scale proteomic studies were performed in mouse models, the studies focused only on the association between diabetes and the nondiabetic control model.[30] To obtain an extended overview of the mechanisms linking obesity/prediabetes to obesity/diabetes, we applied an iTRAQ proteomics strategy to profile obese diabetic ZDF versus obese prediabetic ZF versus control ZL rats.

Several obesity-associated T2D studies using the Zucker rat model[21,41] report that obese ZF and ZDF rats show increased compensatory insulin secretion compared to the ZL rat, and the insulin content of islets is dramatically reduced in the ZDF islet compared to the ZF and ZL islets; the insulin mRNA level is also down-regulated. In this study, Western blot analysis for insulin in Zucker rat islets subjected to iTRAQ analysis revealed a stepwise reduction in ZL, ZF, and, ZDF rat islet; this outcome was consistent with findings of other studies.[41,42] Moreover, the iTRAQ results implied that the expression levels of insulin-1 and insulin-2 were dramatically reduced, giving iTRAQ ratios of 0.43 and 0.52, respectively, in ZDF versus ZL rats (Supplementary Tables S2, S3). Eventually, the reduction of the insulin content in the ZDF islet indicated that the ZDF islet exprerients shows the feature of $\beta$ cell dysfunction and loss.

In this study, the ZF islets also showed changes that were consistent with enlarged $\beta$ cell mass and prediabetic physiological state.[23] The ZF islets respond more efficiently to maintaining normoglycemia in a state of insulin resistance by increasing insulin secretion more than the ZDF islet. Although the OGTT value (193.5 g/dL) is relatively high (demonstrating that our ZF rat model shows a plasma glucose level of prediabetic state), previous studies showed that ZF rats exhibit insulin resistance, high basal glycemia, and abnormal oral glucose tolerance when they are 13 to 14 weeks old.[43] Moreover, we observed that the insulin level after the glucose challenge was dramatically increased only in 14-week-old ZF, while its $\beta$ cell mass increased compared to ZDF and ZL islets. These outcomes imply that ZF islets are an appropriate model for $\beta$ cell compensation for our iTRAQ study.

**Differentially Expressed Proteins in both ZDF and ZF Rats Compared to the ZL Rat.** We analyzed differentially expressed proteins in both obese/diabetic ZDF and obese/prediabetic ZF rats compared to the lean ZL rat to obtain information on obesity-associated proteins. In our iTRAQ data, the largest groups of simultaneously changed proteins in islets of ZDF and ZF rats were involved in both protein metabolism and modification and energy metabolism.

In the functional clustering analysis using the DAVID server,[35] two major views regarding to the protein metabolism and modification were noticed. The first was that several proteins, including elongation factor 1-alpha 1 (Eef1a1),[44] elongation factor 2 (eEF2),[45] and eukaryotic translation initiation factor 5A-1 (Eif5a),[46] along with ribosomal proteins, were involved in protein biosynthesis. Increased levels of these proteins suggested that the proliferation of $\beta$ cells in ZDF and ZF rats was promoted along with obesity in $\beta$ cell compensation, a finding consistent with immunohistochemical analysis. Furthermore, the previous report also suggested that a similar expression pattern of protein biosynthesis-related proteins was observed in an iTRAQ study using the MKR mouse islet.[30] The second view demonstrated that several digestive enzymes and proteases were up-regulated in both ZDF and ZF rats (Supplementary Tables S2, S3). Typically, exopeptidases (carboxypeptidase-like enzyme) and endopeptidases (trypsin-like enzyme) are believed to play important roles in the conversion of proinsulin into insulin and in the intracellular processing of a variety of other precursor forms.[47] In fact, the release and expression of these proteins from the pancreas is closely regulated when maintaining a healthy status. Interestingly, the up-regulated peptidases observed in our iTRAQ data are mostly exocrine proteins excreted from acinar cells. Although finding exocrine proteins in our iTRAQ results may hint at the presence of acinar cells in the islet, the up-regulation of exocrine peptidases may explain $\beta$ cell dysfunction due to the infiltration of exocrine cells to $\beta$ cells of islets.[8] Interestingly, elongation factor 1-alpha 1 (Eef1a1), elongation factor 2 (eEF2), and eukaryotic translation initiation factor 5A-1 have been implicated in the induction of apoptotic cell death, while various peptidases participated in the cell death process.[48−50]

However, significant down-regulation was observed in the proteins involved in energy metabolism. In pancreatic $\beta$ cells, the process of sensing the changes in blood glucose and secretion of the insulin to maintain normoglycemia are controlled by the energy metabolism of $\beta$ cells. The anaplerotic and cataplerotic pathways play an important role to provide metabolic coupling factors that are important for glucose-stimulated insulin secretion (GSIS). Several studies suggested that disruption of this pathway causes the loss of GSIS, thus, leading to $\beta$ cell failure.[11,19] In our iTRAQ results, the proteins included in TCA cycle and glutamate metabolism were down-regulated in both the ZDF and ZF rats. Interestingly, it was reported recently that ZF rats up-regulated glucose metabolism pathways to perform $\beta$ cell compensation.[41] Down-regulation of the ZDF proteins involved in energy metabolism is consistent with our iTRAQ study, whereas down-regulation of the proteins in the ZF rat is different from the previous report.[41] One possible explanation for this inconsistency is that the islet

population used in our iTRAQ is somewhat heterogeneous due to aging and adaptation, especially in the ZF rat.[23] Alternatively, the prediabetic status of the ZF rat was more fully developed and could degenerate some of the ZF islet population, as in ZDF islet, so that the decreased expression of the proteins involved in energy metabolism could occur in the ZF rat.

**Differentially Expressed Proteins in ZDF versus ZF Rats May Link Obesity to T2D.** To obtain insights into the mechanism linking obesity to the development of T2D, analyses of differentially expressed proteins were carried out between ZDF and ZF rats. In this study, we proposed that groups of overexpressed proteins in ZDF rat are associated with $\beta$ cell failure and $\beta$ cell death, while groups of overexpressed proteins in ZF rat are related to $\beta$ cell compensation. The hallmark of diabetes is the specific destruction of pancreatic islet $\beta$ cells; therefore, $\beta$ cell apoptosis is crucial during the progression of diabetes.[51] We have shown that the differentially expressed proteins in the ZDF islet reflected severe insulin resistance or gave rise to complications like hyperglycemia and islet dysfunction, while the proteins identified in the ZF islet associate with a survival factor to prevent $\beta$ cell death and the development of diabetes.

We herein summarize the proteins related with the development of T2D in obese Zucker rat models; these proteins were newly identified from our iTRAQ study. In the Supplementary Discussion, we summarize the proteins identified from our iTRAQ study in obese Zucker rat models; the functions of these proteins were confirmed in our iTRAQ study, but they were previously proposed in other model systems.

**1. Impaired Insulin Secretion.** Reduced expression of the three proteins contributed to the regulation of secretion, vesicle trafficking, and exocytosis, as observed in our iTRAQ data. First, secretogranin II (Scg2) was down-regulated in both ZF and ZDF rats. Secretogranin II (Scg2) is a member of the chromogranin-secretogranin family of proteins, or marker proteins of secretory granules.[52,53] The aggregation of the granin family proteins is dependent on millimolar calcium concentrations and a mildly acidic pH and segregates the regulated cargo from constitutively secreted proteins, while preventing the escape of regulated secretory proteins from immature granules into the constitutive-like secretory pathway.[54]

Second, annexin A2 was dramatically reduced only in the ZDF rat. Annexin A2 is a member of the annexin family of $Ca^{2+}$-regulated, membrane-binding proteins implicated in biochemical and perforated cell experiments in $Ca^{2+}$-triggered exocytosis and endocytosis,[55−57] cell−cell adhesion,[58] and proliferation.[59] Interestingly, the inhibition of annexin A2 expression decreases the cell proliferation rate in p53 apoptotic pathway[60] and induces the negative regulation of exocytosis.

Third, islet of the ZDF rat also displayed a noticeable down-regulation of Rab10 belonging to RAS oncogene family and is present in insulin secretory granules of pancreatic $\beta$ cells.[61] Insulin resistance, the hallmark of T2D, can be caused by impaired GLUT4 biogenesis and trafficking.[62−65] In a key step regulating GLUT4 trafficking, insulin stimulates the translocation of vesicles containing GLUT4 from intracellular compartments to the plasma membrane. Recent studies have showed that the Rab GTPase activating protein AS160, known as a substrate of Akt and Rab10 and a target of AS160, participates in GLUT4 translocation in skeletal muscle and adipose tissue.[66,67] Furthermore, the loss of activity of AS160 and knockdown of Rab10 inhibit GLUT4 translocation, suggesting that they are main regulators in GLUT4 translocation.[67−69] However, GLUT2, an isoform of GLUT4, was predominantly expressed in pancreatic $\beta$ cells, whereas GLUT4 existed mainly in muscle and adipose cells. The relationship between these proteins and GLUT2 is still unclear.

Interestingly, the expression of GLUT4 in pancreatic $\beta$ cells[70] and the role of AS160 associated with $\beta$ cell dysfunction[71] were recently reported. Because Rab10 is a major downstream protein of AS160, the modulation of the expression level of Rab10 is possibly associated with $\beta$ cell dysfunction. Although the Rab10 effect on the translocation of GLUT2 is uncertain, the reduced expression level of Rab10 would result in insulin resistance, contributing to hyperglycemia. The reduced expression of Rab10 in the ZDF islet was reported here for the first time.

**2. Mitochondrial Dysfunction.** Mitochondrial ATP synthase consists of 5 different subunits catalyzes ATP synthesis and utilizes an electrochemical gradient of protons across the inner membrane during oxidative phosphorylation. A recent report showed that the reduced expression of ATP synthase inhibits GSIS in the INS-1 $\beta$ cell line.[72] In our study, two members (Atp5b and Atp5l) of this complex protein were down-regulated in the ZDF rat compared to the ZF rat. The down-regulation of ATP synthase subunit beta (Atp5b), ATP synthase, and the H+ transporting, mitochondrial F0 complex, subunit G (Atp5l) implied that decreased oxidative phosphorylation leads to impaired GSIS and $\beta$ cell dysfunction. Interestingly, no changes in proteins related to oxidative phosphorylation were observed in the ZF rat. Therefore, our data suggested that impaired oxidative phosphorylation is involved in the development of T2D, which is consistent with the MKR proteomics studies.[73]

In addition, our data revealed a marked reduction of Hspd1/Hspe1 (Hsp60/Hsp10 complex); this finding has not been reported in other proteomics studies. Hsp60 functioned in the proper folding of proteins imported to mitochondria and belonged to 13 polypeptides encoded by mitochondrial DNA with ATP hydrolysis.[74] The down-regulation of the Hsp60/Hsp10 chaperone complex suggested that the impaired mitochondrial protein transport and increased misfolded proteins caused the reduction of mitochondrial stability and alteration in mitochondrial functions.

It has been reported that alterations in mitochondrial morphology and metabolism are linked to $\beta$-cell function and survival in vitro.[75−77] In particular, mitochondria in ZDF rat islets undergo such morphological changes, which comprise swelling of the matrix and cristae disruption.[78] In addition, distorted morphology and reduced mitochondrial numbers have been reported in $\beta$-cell mitochondria from diabetic knockout mice,[79] human type 2 diabetic patients,[80] and MKR diabetic islets.[73] Although the mitochondrial dysfunction that we observed is consistent with other proteomics studies,[30,73] it is unclear whether the down-regulation of proteins that are associated with mitochondrial function reflects a reduction in mitochondria or impaired function. The decreased expression of multiple proteins that regulate mitochondrial oxidative function and metabolism presumably resulted from the interplay of decreased mitochondrial function and content. Therefore, additional functional proteomics studies are needed to establish the relationships between the changes in mitochondrial protein expression, morphology, and function during the development of T2D.

**3. Dysregulation of Triglyceride/Free Fatty Acid Cycling and Lipotoxicity.** According to recent studies, both the regulation of triglyceride (TG)/free fatty acid (FFA) cycling and the

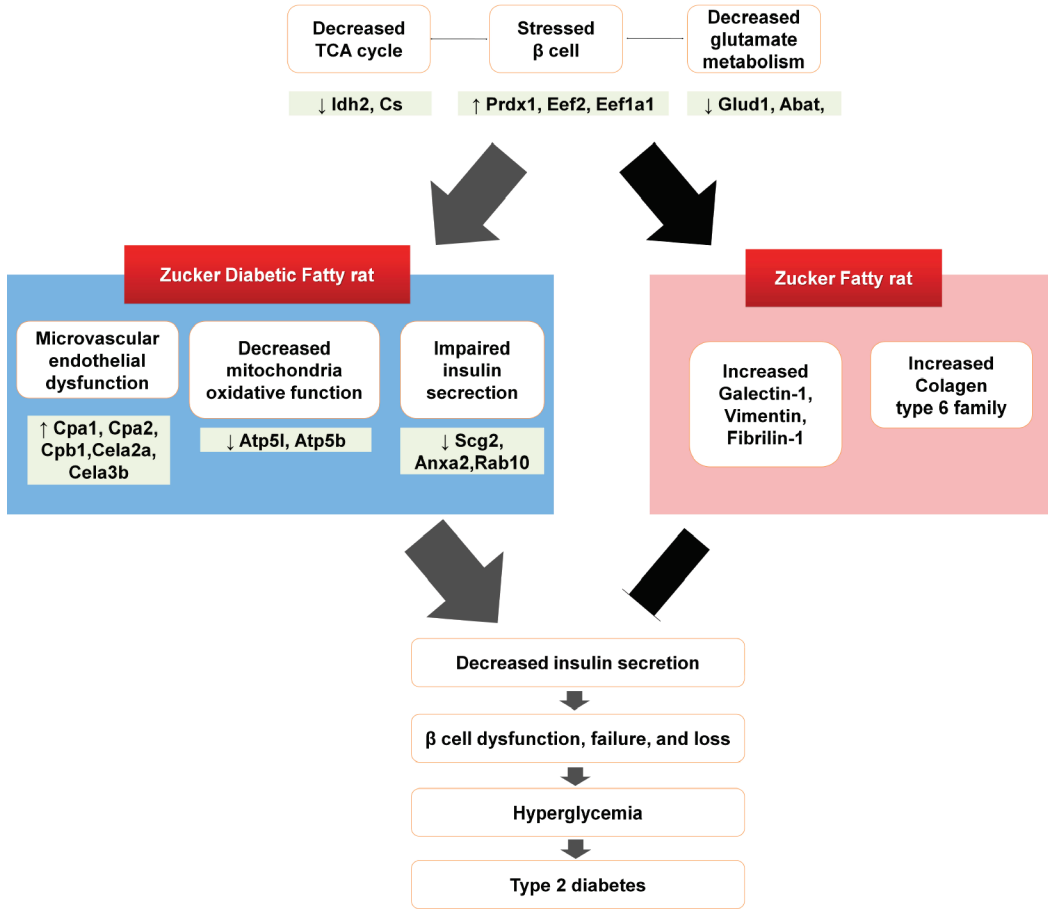


**Figure 6.** A proposed model for differentially expressed proteomes in Zucker Fatty and Zucker Diabetic Fatty rats. The proteins highlighted in the green boxes were significantly differentially expressed proteins that were newly identified in our iTRAQ study using the Zucker rat model.

balance of TG/FFA level have potentially important roles in the islet $\beta$ cell compensation processes and in the protection of islets from damage. In the INS-1 cell line, the overexpression of lipases associated with lipolysis, such as lipoprotein lipase (LPL)[81] and hormone sensitive lipase (HSL),[82] caused impaired GSIS and $\beta$ cell dysfunction. With regard to the INS-1 cell line, $\beta$ cell failure in the ZDF rat is preceded by a rise in plasma nonesterified fatty acid (NEFA) and an accumulation of TG in islets.[21] When pancreatic islets of a normal rat are cultured in the presence of FFA, the TG content increases in islets and GSIS is impaired.[83,84] These findings strongly suggest that the overexpression of lipases and the imbalance in TG/FFA cycling explain the relationship between lipotoxicity and impaired pancreatic $\beta$ cell function. In the present study, we observed that carboxyl ester lipase (Cel) and pancreatic triacylglycerol lipase (Pnlip), known as pancreatic specific lipase, are significantly increased in the ZDF rat compared to the ZF rat. The increased expression of these lipases suggests that the elevated FFA level induced by the lipases results in $\beta$ cell dysfunction and $\beta$ cell apoptosis.

**4. Extracellular Matrix (ECM) Proteins.** Immunohistochemical analysis also showed that the predominant feature of ZF islet is the expansion of the $\beta$ cell mass. Expression of the extracellular matrix proteins is essential for processes such as cell growth, proliferation, development, and fibrosis. Therefore, we expected that proteins related to extracellular matrix would be up-regulated in the ZF rat. But in our iTRAQ data, the expression levels of galectin-1 (Lgal-1), vimentin (Vim), and fibrillin-1 (Fbn1) were increased in the ZF rat compared to the ZDF rat. In addition, we also identified the up-regulation of three collagen type IV family proteins in the ZF rat. Galectin-1,[85] vimentin,[86,87] and fibrillin-1[88] are all associated with cell growth, proliferation, differentiation, and developmental processes in various cell types, and the collagen type IV family proteins are one of the major collagen subtypes at the islet−exocrine interface of the pancreas[89] that are associated with cell growth and proliferation.[90,91] Consequently, the up-regulation of these proteins in the ZF rat could be a benefit for $\beta$ cell compensation and could in turn promote the expansion of the $\beta$ cell mass.

**5. Microvascular Ischemia and Pancreatic Peptidase.** Recently, several studies suggested that pancreatic microvascular endothelial dysfunction and subsequent islet ischemia are the cause of initial dysfunction and subsequent apoptosis of $\beta$ cells in T2D.[92] In our iTRAQ results, the most significantly elevated proteins are exopeptidases and endopeptidases, including carboxylpeptidase, elastase, and chymotrypsinogen. Although the carboxylpeptidase family (Cpa1, Cpa2, and Cpb) and the elastase family (Cela2a and Cela3b) were mostly expressed on pancreatic exocrine cells and secreted into other pancreatic cells or blood, the abundant expression of these peptidases in our iTRAQ analysis using Zucker rat islets indicates that many exocrine cells infiltrate the islets of the ZDF rat and damage $\beta$ cells. In addition, the carboxylpeptidase family[93,94] and the elastase family[95,96] are strongly associated with microvascular endothelial cell dysfunction. Therefore, the up-regulation of

carboxylpeptidase and elastase in the ZDF rat could contribute to $\beta$ cell failure while accelerating microvascular endothelial cell dysfunction.

**Proposed Model in the Development of T2D from Obesity by Comparing the ZDF and ZF Islets.** Both the ZDF and ZF rats exhibited the common phenotype of obesity, insulin resistance, and islet hyperplasia. Furthermore, ZF rats are in a prediabetic state, whereas ZDF rats have overt diabetes. According to our iTRAQ results, both the ZDF and ZF rats showed characteristics of decreased TCA cycle, decreased glutamate metabolism, and stressed islet $\beta$ cells, although corresponding proteins are more down-regulated in ZDF rats for the most part than in ZF rats. It is conceivable that the common proteins for severe diabetic or prediabetic islets are caused by obesity and insulin resistance.

The development of T2D begins with the inability to sustain $\beta$ cell compensation against insulin resistance. In the ZF rat, islet $\beta$ cell compensation for insulin resistance included the expansion of $\beta$ cell mass and hyperinsulinemia, resulting in the long term maintenance of a normal glucose level. However, if there are several factors that lead to susceptible $\beta$ cells, the failure of the compensation process results in T2D. In our iTRAQ study, while the processes for $\beta$ cell failure including decreased mitochondria oxidation, unbalance of TG/FFA cycling, and microvascular endothelial dysfunction were promoted in the ZDF rat, the ZF rat showed significant up-regulation of ECM proteins associated with cell growth and proliferation. These ECM proteins possibly participate in the $\beta$ cell compensation process. Consequently, as proposed in our model (Figure 6), the islet defects including decreased mitochondria oxidation, unbalance of TG/FFA cycling, and microvascular endothelial dysfunction cause a weak link to the $\beta$ cell compensation, thus, promoting $\beta$ cell dysfunction, a progressive reduction in $\beta$ cell number, and hyperglycemia. Once $\beta$ cell dysfunction and hyperglycemia have developed, additional processes linked to glucolipotoxicity and the diabetic milieu result in severe $\beta$ cell failure, $\beta$ cell loss, and overt T2D.

## Conclusions

In obesity-related insulin resistance, failure of $\beta$ cell compensation leads to $\beta$ cell failure. As hyperglycemia is being established, $\beta$ cell failure and loss become more progressive and this leads to the development of obesity-related T2D. Many studies have been performed to explain the mechanism linking the obesity with insulin resistance to T2D. Despite these tremendous efforts, information regarding the obesity-related development of T2D is still sparse.

Using the iTRAQ technique, we have shown for the first time that proteomes in the Zucker Diabetic Fatty rat compared to the Zucker Fatty and the Zucker Lean rat are differentially expressed. To minimize various biases in the experiments using animals and the iTRAQ technique, differentially expressed proteins were identified in three independent biological replicates, based on stringent criteria.

A total of 1084 islet proteins were identified at a >95% confidence level, where 54 and 58 proteins were differentially expressed in the ZDF rat versus the ZL rat and the ZF rat versus the ZL rat, respectively. Furthermore, using functional clustering analysis, we identified novel proteins involved in impaired insulin secretion (Scg2, Anxa2, and Rab10), mitochondrial dysfunction (Atp5b and Atp5l), extracellular matrix proteins (Lgal-1, Vim, and Fbn1), and microvascular ischemia (CPA1, CPA2, CPB, Cela2a, and Cela3b).

Consequently, we propose that impaired insulin secretion, mitochondrial dysfunction, dysregulation of triglyceride/free fatty acid cycling and lipotoxicity, and microvascular dysfunction mediate the progression of obesity-related insulin resistance to the development of T2D, whereas ECM proteins are associated with the $\beta$ cell compensation process. Our novel findings will provide valuable clues to the underlying mechanisms associated with the dynamic transition of obesity to T2D.

**Acknowledgment.** This work was supported by the 21C Frontier Functional Proteomics Project of the Korean Ministry of Science and Technology (grant no. FPR 08-A2-110) and by a grant from the Korean Health 21 R&D Project, Ministry for Health, Welfare and Family Affairs, ROK (A030001, A030003, and 00-PJ3-PG6-GN07-001).

**Supporting Information Available:** (1) Supplementary Methods; (2) Supplementary Discussion; (3) Supplementary Tables: Supplementary Table S1, identified proteins from iTRAQ experiments; Supplementary Table S2, differentially expressed proteins in ZDF versus ZL islets; Supplementary Table S3, differentially expressed proteins in ZF versus ZL islets; Supplementary Table S4, clusters of expression pattern in ZL, ZF, and ZDF rats; (4) Supplementary Figures: Supplementary Figure S1, proteomic profiling of islet proteins from Zucker rat models; Supplementary Figure S2, reproducibility assessment of iTRAQ experiments; Supplementary Figure S3, linear regression analyses on ln-transformed iTRAQ ratios in the three iTRAQ experiments; Supplementary Figure 4, representative Western blot images for differentially expressed proteins in ZL, ZF, and ZDF islets. This material is available free of charge via the Internet at http://pubs.acs.org.

## References

(1) Wild, S.; et al. Global prevalence of diabetes: estimates for the year 2000 and projections for 2030. *Diabetes Care* **2004**, *27* (5), 1047–53.
(2) Centers for Disease Control and Prevention (CDC). Prevalence of overweight and obesity among adults with diagnosed diabetes—United States, 1988−1994 and 1999−2002. *MMWR Morb. Mortal Wkly. Rep.* **2004**, *53* (45), 1066–8.
(3) Reaven, G. M. Banting lecture 1988. Role of insulin resistance in human disease. *Diabetes* **1988**, *37* (12), 1595–607.
(4) Prentki, M.; et al. Malonyl-CoA signaling, lipid partitioning, and glucolipotoxicity: role in beta-cell adaptation and failure in the etiology of diabetes. *Diabetes* **2002**, *51* (Suppl. 3), S405–13.
(5) Leahy, J. L. Pathogenesis of type 2 diabetes mellitus. *Arch. Med. Res.* **2005**, *36* (3), 197–209.
(6) Porte, D., Jr. Clinical importance of insulin secretion and its interaction with insulin resistance in the treatment of type 2 diabetes mellitus and its complications. *Diabetes Metab. Res. Rev.* **2001**, *17* (3), 181–8.
(7) Poitout, V.; Robertson, R. P. Minireview: Secondary beta-cell failure in type 2 diabetes—a convergence of glucotoxicity and lipotoxicity. *Endocrinology* **2002**, *143* (2), 339–42.
(8) Prentki, M.; Nolan, C. J. Islet beta cell failure in type 2 diabetes. *J. Clin. Invest.* **2006**, *116* (7), 1802–12.
(9) Mauvais-Jarvis, F.; Kahn, C. R. Understanding the pathogenesis and treatment of insulin resistance and type 2 diabetes mellitus: what can we learn from transgenic and knockout mice. *Diabetes Metab.* **2000**, *26* (6), 433–48.
(10) Nandi, A.; et al. Mouse models of insulin resistance. *Physiol. Rev.* **2004**, *84* (2), 623–47.
(11) Gembal, M.; Gilon, P.; Henquin, J. C. Evidence that glucose can control insulin release independently from its action on ATP-sensitive K+ channels in mouse B cells. *J. Clin. Invest.* **1992**, *89* (4), 1288–95.
(12) Wollheim, C. B. Beta-cell mitochondria in the regulation of insulin secretion: a new culprit in type II diabetes. *Diabetologia* **2000**, *43* (3), 265–77.

(13) Jensen, M. V.; et al. Metabolic cycling in control of glucose-stimulated insulin secretion. *Am. J. Physiol.: Endocrinol. Metab.* **2008**, *295* (6), E1287–97.
(14) Melloul, D.; Marshak, S.; Cerasi, E. Regulation of insulin gene transcription. *Diabetologia* **2002**, *45* (3), 309–26.
(15) Zhao, L.; et al. The islet beta cell-enriched MafA activator is a key regulator of insulin gene transcription. *J. Biol. Chem.* **2005**, *280* (12), 11887–94.
(16) Bachar, E.; et al. Glucose amplifies fatty acid-induced endoplasmic reticulum stress in pancreatic beta-cells via activation of mTORC1. *PLoS One* **2009**, *4* (3), e4954.
(17) Poitout, V.; Robertson, R. P. Glucolipotoxicity: fuel excess and beta-cell dysfunction. *Endocr. Rev.* **2008**, *29* (3), 351–66.
(18) Cockburn, B. N.; et al. Changes in pancreatic islet glucokinase and hexokinase activities with increasing age, obesity, and the onset of diabetes. *Diabetes* **1997**, *46* (9), 1434–9.
(19) Liu, Y. Q.; Jetton, T. L.; Leahy, J. L. beta-Cell adaptation to insulin resistance. Increased pyruvate carboxylase and malate-pyruvate shuttle activity in islets of nondiabetic Zucker fatty rats. *J. Biol. Chem.* **2002**, *277* (42), 39163–8.
(20) Clark, J. B.; Palmer, C. J.; Shaw, W. N. The diabetic Zucker fatty rat. *Proc. Soc. Exp. Biol. Med.* **1983**, *173* (1), 68–75.
(21) Lee, Y.; et al. Beta-cell lipotoxicity in the pathogenesis of non-insulin-dependent diabetes mellitus of obese rats: impairment in adipocyte-beta-cell relationships. *Proc. Natl. Acad. Sci. U.S.A.* **1994**, *91* (23), 10878–82.
(22) Tokuyama, Y.; et al. Evolution of beta-cell dysfunction in the male Zucker diabetic fatty rat. *Diabetes* **1995**, *44* (12), 1447–57.
(23) Jones, H. B.; Nugent, D.; Jenkins, R. Variation in characteristics of islets of Langerhans in insulin-resistant, diabetic and non-diabetic-rat strains. *Int. J. Exp. Pathol.* **2010**, *91*, 288–301.
(24) Wang, M. Y.; et al. Overexpression of leptin receptors in pancreatic islets of Zucker diabetic fatty rats restores GLUT-2, glucokinase, and glucose-stimulated insulin secretion. *Proc. Natl. Acad. Sci. U.S.A.* **1998**, *95* (20), 11921–6.
(25) De Feyter, H. M.; et al. Early or advanced stage type 2 diabetes is not accompanied by in vivo skeletal muscle mitochondrial dysfunction. *Eur. J. Endocrinol.* **2008**, *158* (5), 643–53.
(26) Ahmed, M.; et al. Proteomic analysis of human adipose tissue after rosiglitazone treatment shows coordinated changes to promote glucose uptake. *Obesity* **2010**, *18* (1), 27–34.
(27) Hwang, H.; et al. Proteomics analysis of human skeletal muscle reveals novel abnormalities in obesity and type 2 diabetes. *Diabetes* **2010**, *59* (1), 33–42.
(28) Deng, W. J.; et al. Proteome, phosphoproteome, and hydroxyproteome of liver mitochondria in diabetic rats at early pathogenic stages. *Mol. Cell. Proteomics* **2010**, *9* (1), 100–16.
(29) Kriegel, T. M.; et al. Identification of diabetes- and obesity-associated proteomic changes in human spermatozoa by difference gel electrophoresis. *Reprod. BioMed. Online* **2009**, *19* (5), 660–70.
(30) Lu, H.; et al. The identification of potential factors associated with the development of type 2 diabetes: a quantitative proteomics approach. *Mol Cell Proteomics* **2008**, *7* (8), 1434–51.
(31) Ross, P. L.; et al. Multiplexed protein quantitation in Saccharomyces cerevisiae using amine-reactive isobaric tagging reagents. *Mol. Cell. Proteomics* **2004**, *3* (12), 1154–69.
(32) Pierce, A.; et al. Eight-channel iTRAQ enables comparison of the activity of six leukemogenic tyrosine kinases. *Mol. Cell. Proteomics* **2008**, *7* (5), 853–63.
(33) American Diabetes Association. Diagnosis and classification of diabetes mellitus. *Diabetes Care* **2010**, *33* (Suppl. 1), S62–9.
(34) Shilov, I. V.; et al. The Paragon Algorithm, a next generation search engine that uses sequence temperature values and feature probabilities to identify peptides from tandem mass spectra. *Mol. Cell. Proteomics* **2007**, *6* (9), 1638–55.
(35) Huang da, W.; Sherman, B. T.; Lempicki, R. A. Systematic and integrative analysis of large gene lists using DAVID bioinformatics resources. *Nat. Protoc.* **2009**, *4* (1), 44–57.
(36) Carbon, S.; et al. AmiGO: online access to ontology and annotation data. *Bioinformatics* **2009**, *25* (2), 288–9.
(37) de Hoon, M. J.; et al. Open source clustering software. *Bioinformatics* **2004**, *20* (9), 1453–4.
(38) Saldanha, A. J. Java Treeview—extensible visualization of microarray data. *Bioinformatics* **2004**, *20* (17), 3246–8.
(39) Rosenbloom, A. L.; et al. Type 2 diabetes in children and adolescents. *Pediatr. Diabetes* **2009**, *10* (Suppl. 12), 17–32.
(40) Nadler, S. T.; et al. The expression of adipogenic genes is decreased in obesity and diabetes mellitus. *Proc. Natl. Acad. Sci. U.S.A.* **2000**, *97* (21), 11371–6.
(41) Nolan, C. J.; et al. Beta cell compensation for insulin resistance in Zucker fatty rats: increased lipolysis and fatty acid signalling. *Diabetologia* **2006**, *49* (9), 2120–30.
(42) Zhou, Y. P.; et al. Basal insulin hypersecretion in insulin-resistant Zucker diabetic and Zucker fatty rats: role of enhanced fuel metabolism. *Metabolism* **1999**, *48* (7), 857–64.
(43) Ionescu, E.; Sauter, J. F.; Jeanrenaud, B. Abnormal oral glucose tolerance in genetically obese (fa/fa) rats. *Am. J. Physiol.* **1985**, *248* (5 Pt. 1), E500–6.
(44) Howe, J. G.; Hershey, J. W. Translational initiation factor and ribosome association with the cytoskeletal framework fraction from HeLa cells. *Cell* **1984**, *37* (1), 85–93.
(45) Weinberg, R. A. E2F and cell proliferation: a world turned upside down. *Cell* **1996**, *85* (4), 457–9.
(46) Cracchiolo, B. M.; et al. Eukaryotic initiation factor 5A-1 (eIF5A-1) as a diagnostic marker for aberrant proliferation in intraepithelial neoplasia of the vulva. *Gynecol. Oncol.* **2004**, *94* (1), 217–22.
(47) Hutton, J. C. Insulin secretory granule biogenesis and the proinsulin-processing endopeptidases. *Diabetologia* **1994**, *37* (Suppl 2), S48–56.
(48) Borradaile, N. M.; et al. A critical role for eukaryotic elongation factor 1A-1 in lipotoxic cell death. *Mol. Biol. Cell* **2006**, *17* (2), 770–8.
(49) Boyce, M.; et al. A pharmacoproteomic approach implicates eukaryotic elongation factor 2 kinase in ER stress-induced cell death. *Cell Death Differ.* **2008**, *15* (3), 589–99.
(50) Hopkins, M. T.; et al. Eukaryotic translation initiation factor 5A is involved in pathogen-induced cell death and development of disease symptoms in Arabidopsis. *Plant Physiol.* **2008**, *148* (1), 479–89.
(51) Mathis, D.; Vence, L.; Benoist, C. beta-Cell death during progression to diabetes. *Nature* **2001**, *414* (6865), 792–8.
(52) Huttner, W. B.; Gerdes, H.H.; Rosa, P. The granin (chromogranin/secretogranin) family. *Trends Biochem. Sci.* **1991**, *16* (1), 27–30.
(53) Taupenot, L.; Harper, K. L.; O'Connor, D. T. The chromogranin-secretogranin family. *N. Engl. J. Med.* **2003**, *348* (12), 1134–49.
(54) Arvan, P.; Castle, D. Sorting and storage during secretory granule biogenesis: looking backward and looking forward. *Biochem. J.* **1998**, *332* (Pt. 3), 593–610.
(55) Chasserot-Golaz, S.; et al. Annexin II in exocytosis: catecholamine secretion requires the translocation of p36 to the subplasmalemmal region in chromaffin cells. *J. Cell Biol.* **1996**, *133* (6), 1217–36.
(56) Creutz, C. E. The annexins and exocytosis. *Science* **1992**, *258* (5084), 924–31.
(57) Sarafian, T.; et al. The participation of annexin II (calpactin I) in calcium-evoked exocytosis requires protein kinase C. *J. Cell Biol.* **1991**, *114* (6), 1135–47.
(58) Mai, J.; Waisman, D. M.; Sloane, B. F. Cell surface complex of cathepsin B/annexin II tetramer in malignant progression. *Biochim. Biophys. Acta* **2000**, *1477* (1−2), 215–30.
(59) Chiang, Y.; et al. Specific down-regulation of annexin II expression in human cells interferes with cell proliferation. *Mol. Cell. Biochem.* **1999**, *199* (1−2), 139–47.
(60) Huang, Y.; et al. Involvement of Annexin A2 in p53 induced apoptosis in lung cancer. *Mol. Cell. Biochem.* **2008**, *309* (1−2), 117–23.
(61) Brunner, Y.; et al. Proteomics analysis of insulin secretory granules. *Mol. Cell. Proteomics* **2007**, *6* (6), 1007–17.
(62) Tilg, H.; Moschen, A. R. Insulin resistance, inflammation, and non-alcoholic fatty liver disease. *Trends Endocrinol. Metab.* **2008**, *19* (10), 371–9.
(63) Guilherme, A.; et al. Adipocyte dysfunctions linking obesity to insulin resistance and type 2 diabetes. *Nat. Rev. Mol. Cell Biol.* **2008**, *9* (5), 367–77.
(64) Muoio, D. M.; Newgard, C. B. Obesity-related derangements in metabolic regulation. *Annu. Rev. Biochem.* **2006**, *75*, 367–401.
(65) Wellen, K. E.; Hotamisligil, G. S. Inflammation, stress, and diabetes. *J. Clin. Invest.* **2005**, *115* (5), 1111–9.
(66) Huang, S.; Czech, M. P. The GLUT4 glucose transporter. *Cell Metab.* **2007**, *5* (4), 237–52.
(67) Sano, H.; et al. Rab10 in insulin-stimulated GLUT4 translocation. *Biochem. J.* **2008**, *411* (1), 89–95.
(68) Sano, H.; et al. Rab10, a target of the AS160 Rab GAP, is required for insulin-stimulated translocation of GLUT4 to the adipocyte plasma membrane. *Cell Metab.* **2007**, *5* (4), 293–303.
(69) Sano, H.; et al. Insulin-stimulated phosphorylation of a Rab GTPase-activating protein regulates GLUT4 translocation. *J. Biol. Chem.* **2003**, *278* (17), 14599–602.

(70) Kobayashi, H.; et al. Expression of glucose transporter 4 in the human pancreatic islet of Langerhans. *Biochem. Biophys. Res. Commun.* **2004**, *314* (4), 1121–5.
(71) Bouzakri, K.; et al. Rab GTPase-activating protein AS160 is a major downstream effector of protein kinase B/Akt signaling in pancreatic beta-cells. *Diabetes* **2008**, *57* (5), 1195–204.
(72) Yang, J.; et al. Leucine culture reveals that ATP synthase functions as a fuel sensor in pancreatic beta-cells. *J. Biol. Chem.* **2004**, *279* (52), 53915–23.
(73) Lu, H.; et al. Molecular and metabolic evidence for mitochondrial defects associated with beta-cell dysfunction in a mouse model of type 2 diabetes. *Diabetes* **2010**, *59* (2), 448–59.
(74) Ostermann, J.; et al. Protein folding in mitochondria requires complex formation with hsp60 and ATP hydrolysis. *Nature* **1989**, *341* (6238), 125–30.
(75) Twig, G.; et al. Fission and selective fusion govern mitochondrial segregation and elimination by autophagy. *EMBO J.* **2008**, *27* (2), 433–46.
(76) Molina, A. J.; et al. Mitochondrial networking protects beta-cells from nutrient-induced apoptosis. *Diabetes* **2009**, *58* (10), 2303–15.
(77) Park, K. S.; et al. Selective actions of mitochondrial fission/fusion genes on metabolism-secretion coupling in insulin-releasing cells. *J. Biol. Chem.* **2008**, *283* (48), 33347–56.
(78) Higa, M.; et al. Troglitazone prevents mitochondrial alterations, beta cell destruction, and diabetes in obese prediabetic rats. *Proc. Natl. Acad. Sci. U.S.A.* **1999**, *96* (20), 11513–8.
(79) Silva, J. P.; et al. Impaired insulin secretion and beta-cell loss in tissue-specific knockout mice with mitochondrial diabetes. *Nat. Genet.* **2000**, *26* (3), 336–40.
(80) Anello, M.; et al. Functional and morphological alterations of mitochondria in pancreatic beta cells from type 2 diabetic patients. *Diabetologia* **2005**, *48* (2), 282–9.
(81) Pappan, K. L.; et al. Pancreatic beta-cell lipoprotein lipase independently regulates islet glucose metabolism and normal insulin secretion. *J. Biol. Chem.* **2005**, *280* (10), 9023–9.
(82) Winzell, M. S.; et al. Pancreatic beta-cell lipotoxicity induced by overexpression of hormone-sensitive lipase. *Diabetes* **2003**, *52* (8), 2057–65.
(83) Unger, R. H. Lipotoxicity in the pathogenesis of obesity-dependent, NIDDM. Genetic and clinical implications. *Diabetes* **1995**, *44* (8), 863–70.
(84) Shimabukuro, M.; et al. Fatty acid-induced beta cell apoptosis: a link between obesity and diabetes. *Proc. Natl. Acad. Sci. U.S.A.* **1998**, *95* (5), 2498–502.
(85) Sakaguchi, M.; et al. A carbohydrate-binding protein, Galectin-1, promotes proliferation of adult neural stem cells. *Proc. Natl. Acad. Sci. U.S.A.* **2006**, *103* (18), 7112–7.
(86) Olson, E. N.; Capetanaki, Y. G. Developmental regulation of intermediate filament and actin mRNAs during myogenesis is disrupted by oncogenic ras genes. *Oncogene* **1989**, *4* (7), 907–13.
(87) Capetanaki, Y.; Smith, S.; Heath, J. P. Overexpression of the vimentin gene in transgenic mice inhibits normal lens cell differentiation. *J. Cell Biol.* **1989**, *109* (4 Pt 1), 1653–64.
(88) Porst, M.; et al. Fibrillin-1 regulates mesangial cell attachment, spreading, migration and proliferation. *Kidney Int.* **2006**, *69* (3), 450–6.
(89) Hughes, S. J.; et al. Characterisation of collagen VI within the islet-exocrine interface of the human pancreas: implications for clinical islet isolation. *Transplantation* **2006**, *81* (3), 423–6.
(90) Naugle, J. E.; et al. Type VI collagen induces cardiac myofibroblast differentiation: implications for postinfarction remodeling. *Am. J. Physiol.: Heart Circ. Physiol.* **2006**, *290* (1), H323–30.
(91) Howell, S. J.; Doane, K. J. Type VI collagen increases cell survival and prevents anti-beta 1 integrin-mediated apoptosis. *Exp. Cell Res.* **1998**, *241* (1), 230–41.
(92) Tal, M. G. Type 2 diabetes: Microvascular ischemia of pancreatic islets. *Med. Hypotheses* **2009**, *73* (3), 357–8.
(93) Hadkar, V.; et al. Carboxypeptidase-mediated enhancement of nitric oxide production in rat lungs and microvascular endothelial cells. *Am. J. Physiol.: Lung Cell Mol. Physiol.* **2004**, *287* (1), L35–45.
(94) Guimaraes, A. H.; et al. TAFI and pancreatic carboxypeptidase B modulate in vitro capillary tube formation by human microvascular endothelial cells. *Arterioscler., Thromb., Vasc. Biol.* **2007**, *27* (10), 2157–62.
(95) Carden, D.; et al. Neutrophil elastase promotes lung microvascular injury and proteolysis of endothelial cadherins. *Am. J. Physiol.* **1998**, *275* (2 Pt. 2), H385–92.
(96) Jaffray, C.; et al. Pancreatic elastase activates pulmonary nuclear factor kappa B and inhibitory kappa B, mimicking pancreatitis-associated adult respiratory distress syndrome. *Surgery* **2000**, *128* (2), 225–31.

PR100759A